Supplementary methods: Image quality assessment of 40-80 keV VMIs (+) and PEI (M_0.4)

Subjective image quality assessment

Those 40-80 keV VMIs (+) and PEI data were independently analyzed by two radiologists with 10 and 20 years of experience in head and neck imaging interpretation, respectively. The evaluation of subjective image quality focused on overall image quality and demarcation of lesion margins. Overall image quality was classified using a 5-point Likert scale (1, unacceptable; 2, suboptimal; 3, adequate; 4, good; 5, excellent). Demarcation of lesion margin was classified using a 5-point Likert scale (ranging from 1 = no visual demarcation to 5 = perfect demarcation of contours).

Objective image quality assessment

Two radiologists (with 7 and 15 years of experience in head and neck imaging interpretation, respectively) blinded to any clinical information and pathological outcomes assessed the signal-to-noise ratio (SNR) and contrast-to-noise ratio (CNR) on the 40-80 keV VMIs (+) and PEI. Regions of interest (ROI) were placed on the following regions: primary tumor, right sternocleidomastoid muscle and pharyngeal air in contrast enhanced phase images, excluding any area of gross necrosis. Quantitative image quality was calculated as the following formulas:

$SNR = HU_{primary\ tumor} / SD_{air}$

$CNR = (HU_{primary\ tumor} - HU_{right\ sternocleidomastoid\ muscle}) / SD_{air}$

$HU_{primary\ tumor}$ and $HU_{right\ sternocleidomastoid\ muscle}$ are defined as the attenuation values of primary tumor and right sternocleidomastoid muscle, respectively. SD_{air} is defined as the standard deviation of attenuation values in pharyngeal air.

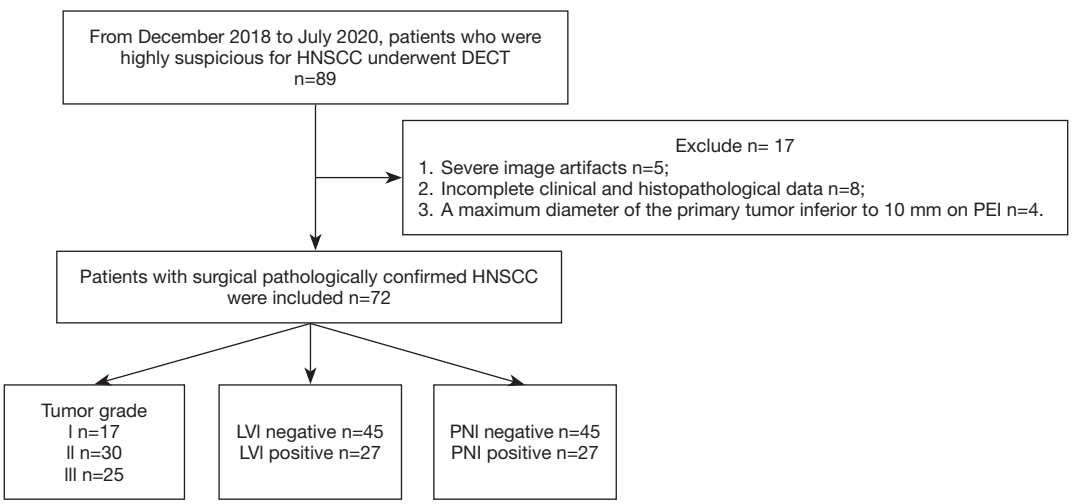

Figure S1 Flowchart shows the strategy for screening patients in this study.

https://dx.doi.org/10.21037/qims-21-650

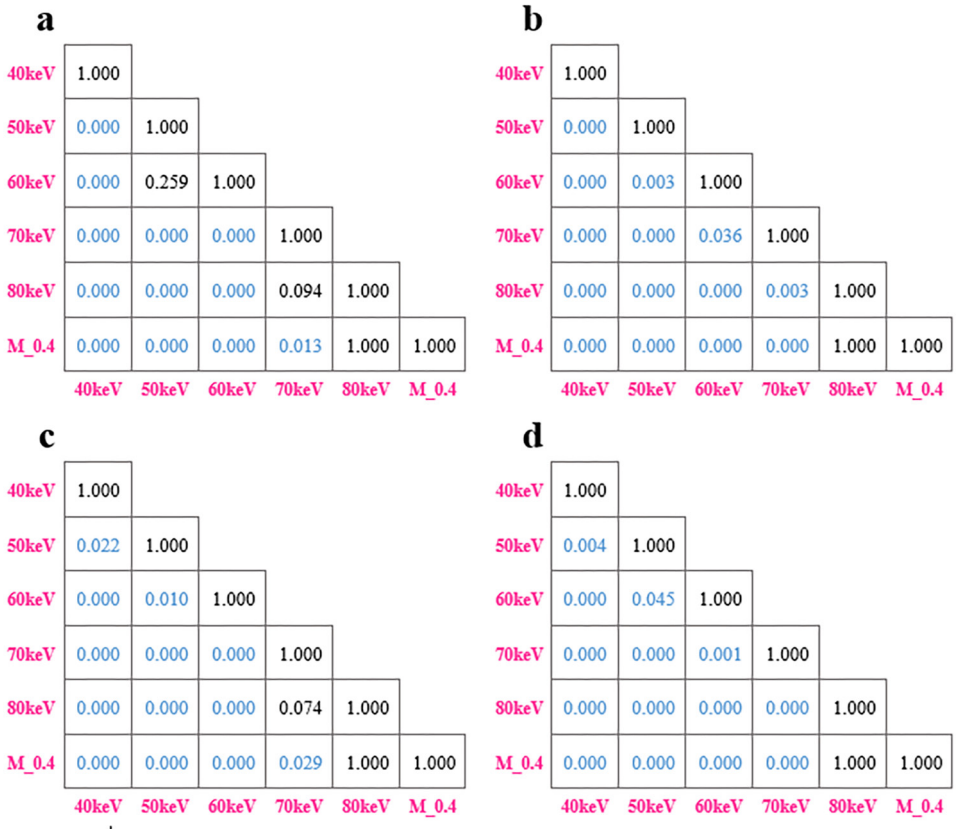

Figure S2 The adjusted P values of pairwise comparison for overall image quality scores (a), demarcation of lesion margins scores (b), signal-to-noise ratio (c) and contrast-to-noise ratio (d) in 40-80KeV VMIs (+) and PEI (M_0.4).

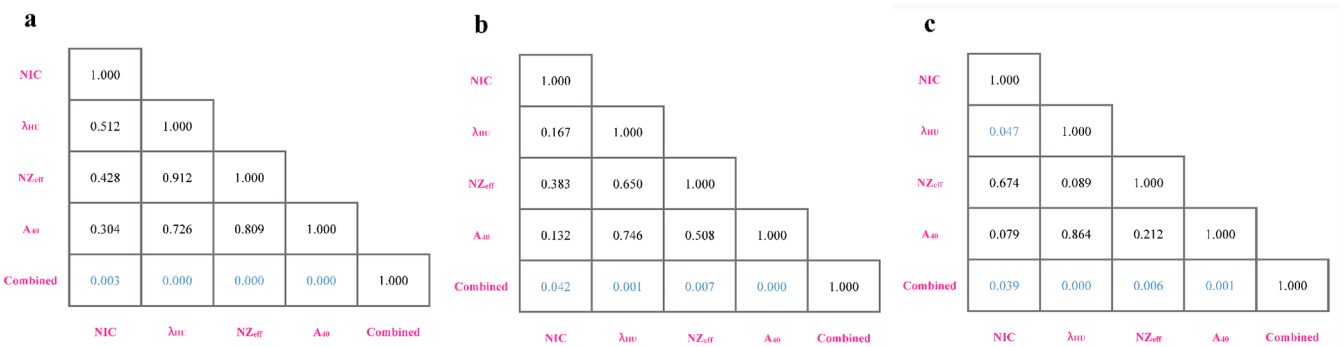

Figure S3 The Delong test results to compare these AUCs of quantitative parameters derived from dual-energy CT for predicting tumor grade (a), lymphovascular invasion (b) and perineural invasion (c).

https://dx.doi.org/10.21037/qims-21-650

Table S1 Subjective image quality assessment for 40-80 keV VMIs (+) and PEI (M_0.4)

Score	40keV	50keV	60keV	70keV	80keV	M_0.4	P value†
Overall image quality							
1	0	0	0	0	1	1	
2	0	0	1	16	18	23	
3	4	17	34	43	51	46	
4	26	36	19	5	2	2	
5	42	19	18	8	0	0	
Total	326	290	270	221	198	193	
Mean ± sd	4.5±0.6	4.0±0.7	3.8±0.9	3.1±0.9	2.8±0.5	2.7±0.6	<0.001
Demarcation of lesion margins							
1	0	0	0	0	0	0	
2	0	0	2	3	10	17	
3	0	16	24	37	50	39	
4	27	34	45	32	12	16	
5	45	22	3	0	0	0	
Total	333	294	271	245	218	215	
Mean ± sd	4.6±0.5	4.1±0.7	3.7±0.5	3.4±0.6	3.0±0.6	3.0±0.7	<0.001

Note. VMI (+) = noise-optimized virtual monoenergetic image; PEI (M_0.4) = 0.4-average-weighted polyenergetic images. †The One-way ANOVA with Bonferroni post hoc test.

Table S2 Objective image quality assessment for 40-80 keV VMIs (+) and PEI (M_0.4)

	40keV	50keV	60keV	70keV	80keV	M_0.4	P value†
SNR	27.24 (26.11–29.86)	22.48 (21.54–25.21)	19.06 (18.15–20.47)	14.36 (12.74–16.33)	12.28 (10.71–13.85)	12.00 (10.73–13.41)	< 0.001
CNR	11.27 (10.47–12.42)	8.76 (8.30–9.68)	7.02 (6.59–7.85)	4.24 (3.61–4.96)	2.02 (1.50–2.88)	2.00 (1.68 – 2.67)	< 0.001

Note. VMI (+) = noise-optimized virtual monoenergetic image; PEI (M_0.4) = 0.4-average-weighted polyenergetic images; SNR: signal contrast-to-noise ratio. CNR: contrast-to-noise ratio. †The Non-parametric Kruskal-Wallis with Bonferroni post hoc test.

https://dx.doi.org/10.21037/qims-21-650

Table S3 Morphological features on 40keV in HNSCC with different histological features

Morphological features	Tumor grade		P value	Lymphovascular invasion		P value	Perineural invasion		P value
	Grade I and II (n=47)	Grade III (n=25)		Negative (n=45)	Positive (n=27)		Negative (n = 48)	Positive (n = 24)	
Inhomogeneity density	33/47 (66.0 %)	22/25 (88.0 %)	0.082	34/45 (75.6%)	21/27 (77.8 %)	0.830	35/48 (72.9 %)	20/24 (83.3 %)	0.327
Ill-defined margins	21/47 (44.7 %)	17/25 (68.0 %)	0.054	21/45 (46.7 %)	17/27 (63.0 %)	0.180	23/48 (47.9 %)	15/24 (62.5 %)	0.243
Infiltration of adjacent structures	19/47 (40.4 %)	16/25 (64.0 %)	0.057	18/45 (40.0 %)	17/27 (63.0 %)	0.059	22/48 (45.8 %)	13/24 (54.2 %)	0.505
Degree of enhancement									
high	13/47 (27.7 %)	11/25 (44.0 %)	0.161	12/45 (26.7 %)	12/27 (44.4 %)	0.121	14/48 (29.2 %)	10/24 (41.7 %)	0.289
intermediate	27/47 (57.4 %)	11/25 (44.0 %)	0.277	25/45 (55.6 %)	13/27 (48.1 %)	0.542	28/48 (58.3 %)	10/24 (41.7 %)	0.182
low	7/47 (14.9 %)	3/25 (12.0 %)	0.735	6/45 (13.3 %)	4/27 (14.8 %)	0.860	7/48 (14.6 %)	3/24 12.5 %)	0.810

https://dx.doi.org/10.21037/qims-21-650